Turkish Journal of Electrical Engineering & Computer Sciences

http://journals.tubitak.gov.tr/elektrik/

Research Article

Turk J Elec Eng & Comp Sci
(2023) 31: 323 – 341

doi:10.55730/1300-0632.3987

A novel COVID-19 herd immunity-based optimizer for optimal accommodation of solar PV with battery energy storage systems including variation in load and generation

Sumanth PEMMADA*, Nita R PATNE, Divyesh KUMAR, Ashwini MANCHALWAR
Department of Electrical Engineering, Visvesvaraya National Institute of Technology, Nagpur, India

Received: 19.09.2022 • **Accepted/Published Online:** 11.01.2023 • **Final Version:** 23.03.2023

Abstract: The world has now looked towards installing more renewable energy sources type distributed generation (DG), such as solar photovoltaic DG (SPVDG), because of its advantages to the environment and the quality of power supply it produces. However, these sources' optimal placement and size are determined before their accommodation in the power distribution system (PDS). This is to avoid an increase in power loss and deviations in the voltage profile. Furthermore, in this article, solar PV is integrated with battery energy storage systems (BESS) to compensate for the shortcomings of SPVDG as well as the reduction in peak demand. This paper presented a novel coronavirus herd immunity optimizer algorithm for the optimal accommodation of SPVDG with BESS in the PDS. The proposed algorithm is centered on the herd immunity approach to combat the COVID-19 virus. The problem formulation is focused on the optimal accommodation of SPVDG and BESS to reduce the power loss and enhance the voltage profile of the PDS. Moreover, voltage limits, maximum current limits, and BESS charge-discharge constraints are validated during the optimization. Moreover, the hourly variation of SPVDG generation and load profile with seasonal impact is examined in this study. IEEE 33 and 69 bus PDSs are tested for the development of the presented work. The suggested algorithm showed its effectiveness and accuracy compared to different optimization techniques.

Key words: Battery energy storage system, coronavirus herd immunity optimizer, optimization, power loss, solar photovoltaic, voltage profile

1. Introduction

The usage of renewable energy sources (RES) has significantly expanded over the past two decades due to the increase in energy demand and the positive impact of RES on the environment due to lowering the carbon footprint. Moreover, utility companies are encouraged to install these RES at smaller levels in the power distribution system (PDS) owing to the reduction in costs associated with these sources. Furthermore, it is anticipated that RES will constitute a larger portion of the global energy mix in the future than conventional energy sources. Solar PV distributed generation (SPVDG) are primarily incorporated into the PDS because of its accessibility, lower operating costs, and the absence of pollution. However, the SPVDG is intermittent, uncertain, and meets the electrical demand only during daylight hours. Despite this, utility companies have aspiring objectives towards installing of these SPVDGs in the PDS due to the abovementioned environment and economic benefits [1].

In addition, it is required to accommodate the SPVDG type of RES at an optimal location with optimal rating to have greater benefits such as reduction in active power loss (APL), reactive power loss (RPL),

*Correspondence: sumanth.pemmada@students.vnit.ac.in

improvement in the voltage profile, and other technical advantages [2]. The allocation of these DGs in the PDS is a mixed integer nonlinear problem. Several methods in the literature based on deterministic, heuristic, and metaheuristic have been proposed to solve the problem of proper accommodation of these DGs. Mixed integer linear programming [3], a rapid analytical algorithm for multiple DG sizing and placement [4], genetic algorithm (GA) [5], particle swarm optimization (PSO) [6], evolutionary programming [7], water cycle algorithm [8], jaya algorithm [9], enhanced elephant herding algorithm [10], artificial bee colony algorithm (ABC) [11], and hybrid algorithms such as hybrid grey wolf optimizer [12] and crow search algorithm autodrive PSO [13] are developed to determine the optimal place and size of the DGs. Furthermore, various classical and artificial intelligence techniques to solve the allotment problem of DG are reported in detail in [14]. Overall, different technical and economic objectives have been optimized, but the primary objectives considered are related to the APL and voltage deviation (VD) issues.

In general, RES is mainly reliant on weather resources that are intermittent and highly variable. The use of battery energy storage systems (BESS) in conjunction with the RES has acquired significant adoption to lessen the impact of the drawbacks related to RES [15]. Moreover, the BESS has a fast-acting capability, sustainable power supply, and is territorial unconstrained. However, Identifying the optimal size of the BESS is crucial for enhancing the technical benefits offered by BESS [16]. Various strategies have been employed in the literature to determine the optimal size of the BESS. Simulated annealing algorithm [17], a dynamic programming method for peak shaving in [18] to model the day ahead optimal scheduling of BESS, and a hybrid combination of teaching-learning based optimization and ABC algorithm are contemplated to determine the proper sizing of BESS [19]. In addition, the superiority of the proposed method in [19] in comparison with GA and differential evaluation is examined. Moreover, a rider optimization algorithm is presented in [20] for the minimization of APL. Furthermore, an improved harmony search algorithm is developed in [21] for peak load shaving with and without BESS.

Various metaheuristic algorithms have been developed for different optimization problems in the literature. However, for nonlinear and multimodal problems such as optimal allotment of SPVDG and BESS, there is still some window to develop alternative nature-inspired algorithms with intelligent features to address the issues effectively. For example, literary methods, such as genetic algorithm [5], particle swarm optimization [6], Jaya algorithm [9], and grey wolf optimization [12], have been suffering from local optima and population diversity. Because of this, the convergence for the optimal solution is poor. Moreover, the balancing of global exploration and local exploitation during the optimization is crucial to find the global optimal solution for any algorithm, which is missing in some of these methods.

In the present article, a recently developed state-of-the-art nature-guided optimization technique namely, coronavirus herd immunity optimizer (CHIO) [22] has been attempted to solve the planning problem of SPVDG and BESS. Here, in CHIO, eliminating the least performing candidates (or infected candidates which are not improved after some iterations) by generating the candidates from the scratch enhances the population diversity. Hence, the elimination of local optima is successfully achieved. The balancing between global exploration and local exploitation is well established by tuning the algorithm parameters: reproduction rate and maximum age. The objective considered in the present study, which consists of a linear combination of APL and VD, is optimized using this suggested algorithm for the planning problem of PDS.

Firstly, optimal placement and sizing of the DG are implemented for the load when the generation is at peak which is obtained from the seasonal generation profile and secondly, optimal BESS location and size are

determined simultaneously by using the proposed algorithm considering the seasonal variation in both load and SPVDG generation profiles. Moreover, during the optimization process, the BESS energy and power constraints are validated. Furthermore, the optimal scheduling of the BESS for 24 h is determined optimally by choosing the four-hour peak load and off-peak load during the 24-h day. The battery is idle for the remaining hours of the day. One charge-discharge cycle per day is considered in this study to extend the life of the BESS [23]. The performance of the proposed algorithm is compared with the different optimization algorithms.

The main contributions of this article are as follows:

1. The novel COVID-19 virus herd immunity-based optimization algorithm is proposed to determine the near global optimal solution for the optimal planning problem (OPP) of PDS.
2. Novel sensitivity factors are proposed for determining the best potential sites for SPVDG installation. Ratings of SPVDG in the PDS are evaluated using the proposed CHIO method with voltage and current limits as constraints.
3. Simultaneous optimal placement, optimal capacity, and power ratings of BESS in the PDS are determined using the suggested CHIO algorithm along with validation of charge/discharge constraints of BESS.
4. Optimum charge/discharge scheduling of the BESS for 24 h is designed to reduce the peak demand on the system.
5. The minimization of APL and VD in the PDS is modeled for the framework of optimal allotment of SPVDG with BESS considering hourly load and generation with seasonal variation for a year is implemented in this study.
6. Different case studies are examined in the presented work for the OPP of PDS with and without SPVDG and BESS on two test PDSs namely, 33 and 69 IEEE bus systems.

The remaining sections of the article are organized in this sequence: The framework of the problem is defined in Section 2. Section 3 is briefed about the suggested algorithm, and its implementation for optimal allotment of SPVDG and BESS is discussed in Section 4. Furthermore, simulation results and discussions are presented in Section 5. Finally, Section 6 provides the conclusion of the work.

2. Framework of the problem

In this section, the problem formulation, which consists of objectives and constraints is briefly explained. The OPP study of the PDS is carried out here for the curtailment of APL and enhancement of the voltage profile. Furthermore, optimal sizing and siting of SPVDG and BESS are evaluated for the above objectives using the novel proposed CHIO algorithm. During the optimization process, the valid constraints such as voltage min/max limits, current max limits, and BESS charge/discharge, state of charge (SOC) min/max limits are included. Moreover, while optimizing the size of BESS, it is ensured that the charge left in the battery at the end of the day is made equal to the charge left in the battery at the start of the day. This is to maintain the energy balance in the PDS and to have enough energy storage at the start of the next day.

A sample portion of the PDS is displayed in Figure 1. It is assumed that the SPVDG and BESS are optimally placed at bus-p and bus-q with optimal ratings, respectively. In Figure 1, p and q are 'from bus' and 'to bus' of a line-k. Here, the resistance and reactance of the line-k are represented by r_k and x_k, respectively. Moreover, P_p^{DG} and Q_p^{DG} represent real and reactive power generations from SPVDG at bus-p, respectively. Similarly, P_p^L, Q_p^L and P_q^L, Q_q^L are real and reactive power loads at bus-p and bus-q, respectively. Furthermore, P_q^{ch} and P_q^{dch} are charging and discharging powers, respectively through the BESS connected at bus-q (at any time, only either charge or discharge occurred through the BESS). Furthermore, P_p, Q_p and P_q,

Q_q are real and reactive power injections at bus-p and bus-q, respectively. Lastly, $V_p\angle\delta_p$ and $V_q\angle\delta_q$ represent the voltage with phase angle at bus-p and bus-q, respectively.

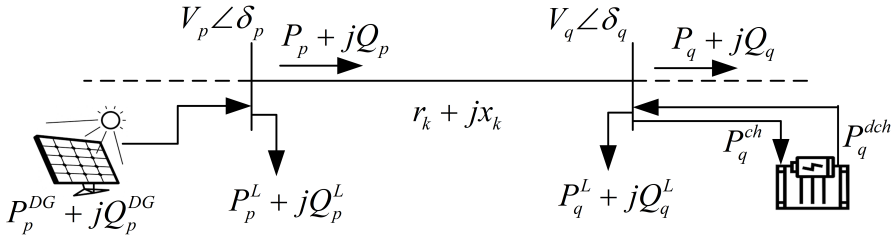

Figure 1. A sample section of a power distribution system.

2.1. Objective function for SPVDG sizing

The objective obj_1, which is the linear combination of APL and VD as shown in Equation (1) is considered for estimating the best position and size of the SPVDG. In this study, weighting factors c_1 and c_2 are considered to be 1 based on the work reported in [23]. Moreover, these weights are assumed to be the same for all the cases studied in the presented manuscript. In general, the PDS operator assigns the weights c_1 and c_2 in real-time operation based on the requirements and relative importance of the objectives pertaining to the safety and appropriate functioning of the PDS. In Equations (1) and (2), PL represents the total APL of the PDS. PL^{DG} and PL^{base} are APL of the PDS with and without SPVDG, respectively. Similarly, V_p^{DG} and V_p^{base} are voltages at bus-p with and without SPVDG in the PDS, respectively. Moreover, the number of lines and number of buses of the PDS are denoted by $Nline$ and $Nbus$, respectively.

$$obj_1 = c_1 \times \frac{PL^{DG}}{PL^{base}} + c_2 \times \frac{\sum_{p=2}^{Nbus}\left(V_p^{DG}-1\right)^2}{\sum_{p=2}^{Nbus}\left(V_p^{base}-1\right)^2} \tag{1}$$

$$PL = \sum_{k=1}^{Nline}\left|V_p\angle\delta_p\left(\frac{V_p\angle\delta_p - V_q\angle\delta_q}{r_k + jx_k}\right)^* + V_q\angle\delta_q\left(\frac{V_q\angle\delta_q - V_p\angle\delta_p}{r_k + jx_k}\right)^*\right| \tag{2}$$

2.2. Objective function for BESS sizing

The sizing of the BESS (i.e. determining the optimal energy rating and power rating) involved estimating the optimal hourly charge-discharge scheduling of the BESS over 24 h using the CHIO algorithm. Therefore, the overall objective obj_2, considering APL and VD, is slightly modified as in Equation (3), where $PL_t^{DG\_BESS}$ represents the total APL of the system considering both SPVDG and BESS placed in the PDS at a time slot-t, whereas the APL of the PDS without any external device (i.e. base case) at a time slot-t is represented by PL_t^{base}. Similarly, $V_{t,p}^{base}$ and $V_{t,p}^{DG\_BESS}$ denote the voltage at the bus-p at a time slot-t for the base case and for the case with SPVDG and BESS, respectively. Lastly, the total number of time slots is represented by

Ts.

$$obj_2 = c_1 \times \frac{\sum_{t=1}^{Ts} PL_t^{DG\_BESS}}{\sum_{t=1}^{Ts} PL_t^{base}} + c_2 \times \frac{\sum_{t=1}^{Ts}\sum_{p=2}^{Nbus}\left(V_{t,p}^{DG\_BESS}-1\right)^2}{\sum_{t=1}^{Ts}\sum_{p=2}^{Nbus}\left(V_{t,p}^{base}-1\right)^2} \tag{3}$$

2.3. Operating constraints

The following constraints are to be satisfied in this work during the optimization of the problem. Violation of any undermentioned operational limits results in an addition of penalty factor to the objective function. As this research is aimed to find a minimum APL and VD as shown in Equations (1) and (3), the penalty factor is set at a higher value (the analysis is done with 20 p.u.).

2.3.1. Power balancing equations

During the load flow, the net active and reactive power (P_p and Q_p) at any bus-p should be zero to meet the power balancing equations as given in Equations (4) and (5), where P_p^{DG}, Q_p^{DG} and P_p^L, Q_p^L are active and reactive powers of DG and demand at bus-p, respectively. $y_{p,q}$, θ_p, and θ_q are the admittance magnitude and angles of the branch amid buses p and q.

$$Net\,P_p = P_p^{DG} - P_p^L + \left(P_p^{dch}\ or\ -P_p^{ch}\right) - V_p \sum_{q=1}^{Nbus} V_q\, y_{p,q} \cos(\delta_p - \delta_q - \theta_p + \theta_q) = 0 \tag{4}$$

$$Net\,Q_p = Q_p^{DG} - Q_p^L - V_p \sum_{q=1}^{Nbus} V_q\, y_{p,q} \sin(\delta_p - \delta_q - \theta_p + \theta_q) = 0 \tag{5}$$

2.3.2. DG unit operational limits

Power injections of the SPVDG into the PDS should be kept in bounds and may be represented as in Equation (6), where P_p^{DGmin}, P_p^{DGmax} are minimum, maximum active power limits of DG units at bus-p. In this study, P_p^{DGmin} and P_p^{DGmax} are 0 and 3 MW, respectively.

$$P_p^{DG\,\min} \le P_p^{DG} \le P_p^{DG\,\max} \tag{6}$$

2.3.3. Voltage bounds at a bus

Bus voltage should be kept within the lowest and maximum limit. This may be represented as in Equation (7), where V_p, V_p^{min}, and V_p^{max} are the voltage magnitude and the lowest and the highest permitted voltages at bus-p, respectively (V_p^{min} and V_p^{max} are considered 0.95 and 1.05 p.u. in this work, respectively).

$$V_p^{\min} \le V_p \le V_p^{\max} \tag{7}$$

2.3.4. Branch current limits

Branch current passing through the branches is to be kept between the maximum and minimum current restrictions as shown in Equation (8). The current and its maximum permissible limit in a line-k are denoted by I_k and $I_{max,k}$ [24].

$$-I_{max,k} \leq I_k \leq I_{\max,k} \tag{8}$$

2.4. Model and constraints of BESS

In this article, the sodium-sulfur (NaS) battery is regarded as a storage device. Despite NaS batteries costing more than standard lead-acid batteries initially, their use is ultimately more cost-effective because of their longer lifespan and higher efficiency, which onsequently reduces operating and maintenance expenses [23]. This study simulated a NaS battery with an average lifespan of six years and an average efficiency of 85% while charging and discharging. The following are the BESS energy equations for charging and discharging:

$$While\ discharging:\ E_b(t) = E_b(t-1) - \frac{P_b(t) \times \Delta t}{\eta_d} \tag{9}$$

$$While\ charging:\ E_b(t) = E_b(t-1) + (P_b(t) \times \Delta t \times \eta_c) \tag{10}$$

Here $E_b(t)$ and $E_b(t-1)$ are energy left in the battery at the end of the hour-t and the previous hour $t-1$, respectively. $P_b(t)$ is the power charge/discharge through the battery during the hour-t. Furthermore, η_c and η_d are efficiencies of the charge and discharge of the battery, respectively. Δt represent the time slot duration. Here Δt is considered to be 1 h. Moreover, while optimizing the accommodation of BESS for the objective in Equation (3), the charging power of the battery is considered a load; similarly, discharging power of the battery is considered a generation at the bus where BESS is located.

In addition, to prolong the life of the battery, it is ensured that the energy left in the battery is kept within the minimum and maximum limits of the SOC at the end of every hour as displayed in Equation (11). Moreover, the number of charge-discharge cycles in a given day is limited to one. Moreover, the energy left in the battery at the end of the day is maintained equal to the initial stored energy in the battery at the start of the day as shown in Equation (12). This is to ensure the energy balance in the system as well as to have enough stored energy in the battery at the start of the next day for peak hours.

$$\left(SOC^{\min} \times E_r\right) \leq E_b(t) \leq \left(SOC^{\max} \times E_r\right) \tag{11}$$

$$E_b(0) = E_b(T) \tag{12}$$

Here E_r is the optimal energy rating of the BESS. SOC^{min} and SOC^{max} are the minimum and maximum SOC of the battery, respectively. In this work, SOC^{min} and SOC^{max} are considered 20% and 90%, respectively. The terms $E_b(0)$ and $E_b(T)$ represent the energy stored in the battery at the start and at the end of the day, respectively (In this work, it is assumed that initial stored energy in the battery is equal to the SOC^{min}). To fulfill the energy constraints of the battery in Equations (11) and (12) during the optimization, $E_b(t)$ may be expressed as in Equation (13).

$$E_b^{\min}(t) \leq E_b(t) \leq E_b^{\max}(t) \tag{13}$$

$$E_b^{\min}(t) = \max \begin{cases} SOC^{\min} \\ E_b(t-1) - P_r \times \Delta t/\eta_d \\ E_b(0) - (T-t) \times P_r \times \Delta t \times \eta_c \end{cases} \tag{14}$$

$$E_b^{\max}(t) = \min \begin{cases} SOC^{\max} \\ E_b(t-1) + P_r \times \Delta t \times \eta_c \\ E_b(0) + (T-t) \times P_r \times \Delta t/\eta_d \end{cases} \tag{15}$$

Here P_r is the optimal power rating of the BESS. Based on the min/max limits on the E_b as in Equation (13), the power charge/discharge min/max limits are defined as in Equation (16).

$$P_b^{\min}(t) \le P_b(t) \le P_b^{\max}(t) \tag{16}$$

Here P_b^{min} and P_b^{max} are defined during the discharge of the BESS as shown in Equations (17) and (18).

$$P_b^{\min}(t) = \max \begin{cases} 0 \\ (E_b(t-1) - E_b^{\max}(t)) \times \eta_d/\Delta t \end{cases} \tag{17}$$

$$P_b^{\max}(t) = \min \begin{cases} \left(E_b(t-1) - E_b^{\min}(t)\right) \times \eta_d/\Delta t \\ P_r \end{cases} \tag{18}$$

Similarly, P_b^{min} and P_b^{max} are defined during the charge of the BESS as shown in Equations (19) and (20).

$$P_b^{\min}(t) = \max \begin{cases} 0 \\ \left(E_b^{\min}(t) - E_b(t-1)\right)/(\eta_c \times \Delta t) \end{cases} \tag{19}$$

$$P_b^{\max}(t) = \min \begin{cases} (E_b^{\max}(t) - E_b(t-1))/(\eta_c \times \Delta t) \\ P_r \end{cases} \tag{20}$$

3. The proposed CHIO algorithm

This work proposed a state-of-the-art human-based nature-guided optimization method viz., coronavirus herd immunity optimizer (CHIO) [22]. The optimization procedure depended on the herd immunity level and social distancing of the society/population when COVID-19 is attacked. The population's immunity level has been classified into three groups when the virus strikes: susceptible, infected, and immune. Susceptible people are those who have not been affected by COVID-19 but may get affected if they come into contact with an infected person. Those with a proven case of the virus are considered to be infected, and they run the risk of spreading it to the susceptible people. People who have successfully recovered from the virus are considered to be immune. This particular group of individuals can halt the virus from spreading further. The proposed algorithm is based on the idea of immunizing a significant proportion of the susceptible population that is not affected to protect the community from the infection in the best possible way.

The concept of achieving herd immunity among the individuals in a society is pictorially represented

in Figure 2. In the initial stage, a larger number of susceptible individuals exist in the community with a few infected individuals. Then, in the second stage, the virus infected more individuals in the community. Moreover, some individuals recovered from the illness and are immune. Furthermore, the virus affected very few individuals to the mortality, and most of the remaining individuals are either recovered (and immune) or susceptible in the last stage.

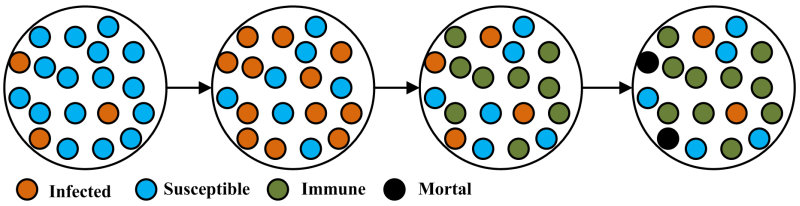

Figure 2. Spreading of the virus and herd immunity in a community.

During the optimization using CHIO, a status vector (S) and an age vector (A) are defined for each individual in the initial population. S takes the value of 0, 1, or 2 (0 = susceptible; 1 = infected; 2 = Immune). However, S is initialized with 'zero' for all the individuals except a very few with 'one' at the start of the iteration. At later iterations/generations, S is updated from 0 to 1 and from 1 to 2 along with the updating individuals. This occurred according to the algorithm updating procedure where social distancing is one of the criteria used to evolve herd immunity in the population. Moreover, A is initialized with 'zero' at the start though, it is incremented by 'one' for every iteration only when the updated candidate is worse than the present candidate. Again, the age vector is reassigned with 'zero' when it reaches the maximum infected case age (AGE_{max}).

Two control parameters are employed in this algorithm: the first is the reproduction rate (RR), which regulates the algorithm by spreading the virus among people. A higher value of RR leads to a high rate of spreading the disease and thus the exploration becomes large. Therefore, the search requires a longer time to converge. On the other hand, when the value of RR is small, the generated candidates which are affected by the virus are fewer and thus the exploration in the search space is less. As a result, the convergence is faster; however, the algorithm may always converge to the local optimum. Therefore, it is crucial to determine the value of RR so that the exploration and exploitation are balancing. In accordance with this, the value of RR is taken as 0.05 by trial and error which empowers the convergence behavior of CHIO to achieve the right balance between exploration and exploitation of the search space and thus the best performance is attained in the presented manuscript. Second, AGE_{max} determines the condition of the infected person, i.e. whether the person has recovered or has become mortal The infected cases that are reached the AGE_{max} threshold without improvement will be destroyed, and a new solution will be rebuilt from scratch. This operation can be considered a source of exploration. The smaller the value of AGE_{max}, the higher the exploration. The value of AGE_{max} taken as 100 in this manuscript seems reasonable to diversify the search. However, there is no significant effect of the value of AGE_{max} on the results produced. Overall, the properly tuned parameters of RR and AGE_{max} produced the near-global optimal solution for the given problem. The algorithm parameters taken in this manuscript are provided in Section 5 in Table 1. The following steps described the working of the CHIO algorithm.

Algorithm 1: Implementation steps for optimization through the CHIO.

1. Initialize the algorithm parameters such as population size (np), maximum iterations ($iter_{max}$), initially

infected individuals (N_0), reproduction rate (RR), age vector (A), and maximum infected case age (AGE_{max}). The objective function $f(x)$ is to be minimized for x in the range of $[l,\ u]$ as shown below, where l and u are lower and upper limits of x, respectively.

$$\min_x f(x)\ \ x \in [l,\ u] \tag{21}$$

2. Generate an initial random population of size np, and estimate the objective value for each candidate. Moreover, the status vector S_i, (where, i=1,2, ... np) is initiated with either 1 or 0 for each candidate in the population (1= infected; 0=susceptible).

3. The i^{th} individual at $iter^{th}$ iteration x_i^{iter}, updated to x_i^{iter+1} at $(iter+1)^{th}$ iteration is dependent on the four categories below.

$$x_i^{iter+1} = \begin{cases} x_i^{iter} & if\ rand \geq RR \\ C\left(x_i^{iter}\right) & if\ 0 < rand < (1/3\ \times RR) \\ N\left(x_i^{iter}\right) & if\ \ (1/3\ \times RR) < rand\ < (2/3\ \times RR) \\ R\left(x_i^{iter}\right) & if\ (2/3\ \times RR) < rand < RR \end{cases} \tag{22}$$

where $rand$ = uniformly distributed random number between 0 and 1, and

$$C\left(x_i^{iter}\right) = x_i^{iter} + rand \times \left(x_i^{iter} - x_c^{iter}\right) \tag{23}$$

$$N\left(x_i^{iter}\right) = x_i^{iter} + rand \times \left(x_i^{iter} - x_n^{iter}\right) \tag{24}$$

$$R\left(x_i^{iter}\right) = x_i^{iter} + rand \times \left(x_i^{iter} - x_r^{iter}\right) \tag{25}$$

where x_c^{iter} and x_n^{iter} are random infected and susceptible cases from the population, such that $c = i|_{S_i=1}$ and $n = i|_{S_i=0}$, respectively. x_r^{iter} is the best candidate from the immune case, such that

$$f(x_r^{iter}) = \arg \min_{i \sim \{|S_0=2\}} f(x^i) \tag{26}$$

4. Forward x_i^{iter+1} to the next iteration, if the fitness of x_i^{iter+1} is better than x_i^{iter}. Otherwise, forward x_i^{iter} to the next iteration and increment the age vector A_i, by one. Further, S_i and A_i are also updated according to the Equation (27). Where $covid_i^{iter+1}$ is a binary number which is equal to 1 when the new candidate x_i^{iter} is generated from the infected candidate. Furthermore, $\Delta f(x^{iter})$ is the average fitness of the population at the $iter^{th}$ iteration.

$$\left.\begin{array}{l} S_i = 1,\ A_i = 1\,;\ \ if\ \ \left(\left(f(x_i^{iter+1}) > \Delta f(x^{iter})\right) \wedge (S_n = 0) \wedge \left(covid_i^{iter+1}\right)\right)\ = True \\ S_i = 2,\ A_i = 0\,;\ \ if\ \ \left(f(x_i^{iter+1}) < \Delta f(x^{iter}) \wedge (S_n = 1)\right) = True \end{array}\right\} \tag{27}$$

5. According to the maximum infected case age (AGE_{max}), if the fitness value of x_i^{iter} does not improve after a certain number of iterations, it is deemed fatal. Hence, the candidate solution x_i^{iter} is recreated amid the lower and upper limits. Moreover, A_i and S_i are initiated to zero. This mechanism is used to improve the

diversity and avoid local optima of the searching algorithm.
6. Check the stopping condition for maximum number of iterations, $iter_{max}$; if not satisfied, follow the steps from 3 to 5.

4. Application of the proposed method for the OPP of PDS

In this section, the proposed CHIO algorithm is utilized to evaluate the optimal solution for the OPP of PDS. At first, the optimal location and sizing of SPVDG are determined. Secondly, optimal siting and sizing of BESS are studied within the presence of SPVDG by the suggested method. The operational constraints as well as battery constraints are considered while solving the whole optimization problem for the objectives shown in Equations (1) and (3).

4.1. Optimal accommodation of SPVDG

In this section, the optimal accommodation of the SPVDG is presented. Here, the CHIO algorithm has been used to identify the optimal rating of the DG in the PDS for curtailing APL and VD. Before optimizing the rating of this unit, its appropriate placement must be determined. Otherwise, the system's performance may suffer. Prior location estimation reduces the search algorithm's computation time for DG size optimization. For the best position of SPVDG, the objective mentioned in Equation (1) is determined using the direct approach load flow method [25]. This objective is evaluated by sequentially injecting thirty percent of the overall active power demand at each node. Once the evaluation is completed for all the nodes in the PDS, the node that gives the minimum value of the objective is selected as the best node (Loc) to place the SPVDG. Moreover, in this work, the normalized load and normalized SPVDG generation profiles are considered for the study as shown in Figures 3a and 3b. The data regarding variation in load and generation are taken from [23]. Here, the typical data for 24 h represented the load and generation data for a particular season. Therefore, the 96 h of data reflected all four distinct seasons that make up a typical year (8760 h): winter, spring, summer, and fall, sequentially. As most of the days in a season follow a similar pattern of demand/generation; Here, a valid assumption is considered regarding the data of demand/generation of a season that comprises an average demand/generation of all days of that season at each hour.

$$P^{L}_{t,p} = loadfraction_t \times P^{L}_{p} \tag{28}$$

$$Q^{L}_{t,p} = loadfraction_t \times Q^{L}_{p} \tag{29}$$

$$P^{DG}_{t,Loc} = genfraction_t \times P^{DG}_{Loc} \tag{30}$$

The hourly active and reactive power load at a bus-p (where p=1,2, ... $Nbus$) is obtained as shown in Equations (28) and (29), where $loadfraction_t$ is the normalized load in p.u. at the hour-t and P^{L}_{p} is the peak load at bus-p. Similarly, hourly generation of the SPVDG at the optimal location (Loc) is obtained from Equation (30), where $genfraction_t$ is the normalized generation of SPVDG at the hour-t and P^{DG}_{Loc} is the optimal size of the SPVDG. This optimal size is determined for peak generation which occurred at $t = 85$ as shown in Figure 3b. Therefore, the load at all buses at the 85^{th} hour using Equations (28) and (29) is considered for estimating the optimal peak size of the SPVDG. Furthermore, the implementation steps for determining

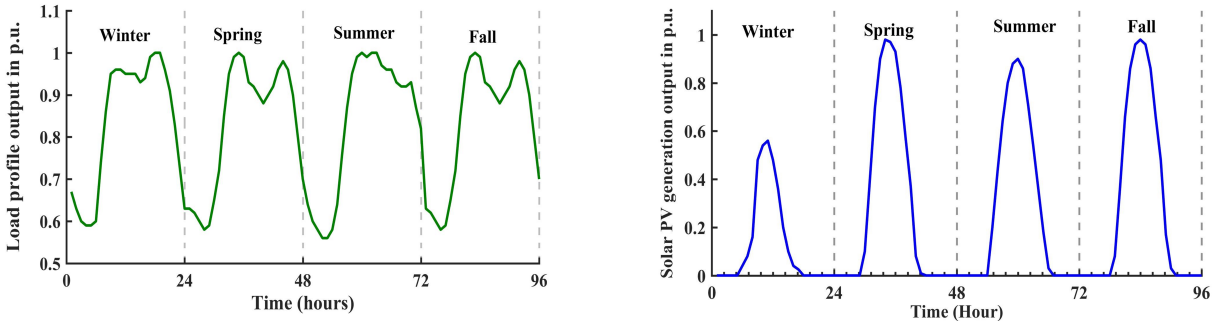

Load SPVDG

Figure 3. Normalized load and SPVDG generation profiles for a year.

the optimal size of the SPVDG while satisfying the operating constraints using the suggested methodology are given in Algorithm 2.

Algorithm 2: Implementation steps for estimating optimal rating of SPVDG by CHIO

1. Read the PDS data, count of DGs (mDG), P^{DGmin}, P^{DGmax}, optimal SPVDG bus location (Loc), and CHIO algorithm parameters such as np, $iter_{max}$, N_0, RR, S, A, and AGE_{max}.
2. Set pop counter, $i = 1$.
3. **while** $i \leq np$ **do**
4. Create mDG number of DG ratings, randomly between P^{DGmin} and P^{DGmax} as $P_{Loc}^{DG} = P_{Loc}^{DG\,\min} + \left(P_{Loc}^{DG\,\max} - P_{Loc}^{DG\,\min}\right) \times rand$. The candidate solution (P_{Loc}^{DG}) size is $1 \times mDG$.
5. Inject P_{Loc}^{DG} as a negative active power load at the locations specified by Loc as shown $P_{Loc}^{L} = P_{Loc}^{L} - P_{Loc}^{DG}$.
6. Evaluate the objective in Equation (1) using the load flow given in [25] and validate the operational constraints from Equations (4) to (8). If the operational constraints are disobeyed, then add a penalty to the Equation (1) accordingly.
7. Update the pop counter, $i = i + 1$.
8. End **while**
9. Set generation counter, $iter = 1$.
10. **while** $iter \leq iter_{max}$ **do**
11. As illustrated in Equation (22) update the population and follow steps 5 to 6 to find the objective in Equation (1).
12. Keep the better candidate solution between present and updated candidate according to the minimum objective. Moreover, update the status vector (S) and age vector (A) according to Equation (27). Further, Determine the candidate that produced the minimum objective and store it as $P_{Loc}^{DG,best}$.
13. Revise the generation count, $iter = iter + 1$.
14. End **while**

4.2. Optimal accommodation of BESS with SPVDG

Once the optimal peak size of the SPVDG is estimated for the reduction of APL and VD using CHIO, the optimal accommodation of BESS is modeled considering the SPVDG in the PDS. The accommodation of BESS constitutes simultaneous siting and sizing of BESS to optimize the objective given in Equation (3). The sizing of the battery involved estimating the optimal energy rating and power rating of the battery. In this work, the

battery is operated for one charge-discharge cycle per day to improve the life of the battery; therefore, it is assumed that the battery is discharged for four hours during the peak-hour period (5 PM to 9 PM) and charged for 4 h during the off-peak hour period (10 AM to 2 PM). Furthermore, the battery is idle for the remaining hours of the day. Due to the charge/discharge of the battery at the off-peak/peak hours, the peak demand on the PDS is reduced. Furthermore, it is maintained that the initial charge left in the battery at the start of the day is the same at the end of the day to ensure the energy balance in the PDS. In addition, while solving for the optimal energy rating and power rating of the battery, the constraints mentioned in Equations (9) to (20) are followed. Moreover, in this work, it is assumed that the charging power is considered to be a load, and discharging power is assumed to be a generation at the bus where the BESS is located. Here, the main goal of the problem is to find the optimal scheduling of charge/discharge power through the battery for 96 h (24 h is a season) for the optimal energy rating and power rating of the battery at the optimal bus location in the PDS. Therefore, solving this problem involves the main problem, i.e. finding the energy and power rating, and a subproblem, i.e. finding the charge/discharge powers of the battery. Moreover, while solving this problem using the CHIO algorithm the objective in Equation (3) is required to be evaluated for each variation in demand/generation for each particle in the population. Therefore, in this work, the variation in demand/generation is considered for 96 h ($24 hours \times 4 seasons$) instead of 8760 hours (24×365) to reduce the computational burden on the algorithm. The implementation steps for the optimal accommodation of BESS in the PDS is described in the Algorithm-3.

Algorithm 3: Implementation steps for optimal accommodation of BESS in the PDS

1. Read the PDS data, battery parameters such as P_r^{min}, P_r^{max}, E_r^{min}, E_r^{max}, η_d, η_c, $E_b(0)(= SOC^{initial})$, and T (=24 h), and CHIO algorithm parameters such as np, $iter_{max}$, N_0, RR, S, A, and AGE_{max}.
2. Set the bus counter, $bc = 1$.
3. Set the main iteration counter, $iter^{main} = 1$.
4. Set the main population counter, $pop^{main} = 1$.
5. Initialize the energy rating (E_r), between E_r^{min} and E_r^{max}; similarly, power rating (P_r), between P_r^{min} and P_r^{max}.
6. Set the sub iteration counter, $iter^{sub} = 1$.
7. Set the sub-population counter, $pop^{sub} = 1$.
8. Set the time slot, $t = 1$.
9. Initialize P_b between P_b^{min} and P_b^{max} using Equations (17) to (20). Moreover, evaluate E_b using Equations (9) and (10).
10. Check $t \leq T$. If yes; update $t = t + 1$, and go to step 9. If no; go to step 11.
11. Run the load flow [25] to evaluate the objective given in Equation (3). While solving the load flow for T_s (= 96 hrs) slots, variation of load and SPVDG generation is followed according to Equations (28) to (30) with peak SPVDG size from Algorithm-2 at the optimal location. Here, BESS is scheduled for a day; therefore, the size of P_b is $1 \times T$ (= 24 hrs), and the same is repeated for all seasons to make up for T_s ($4 \times 24 hrs$) slots.
12. Check $pop^{sub} \leq np$. If yes; update $pop^{sub} = pop^{sub} + 1$ and go to step 8. If no; go to step 13.
13. Update the values of P_b according to the CHIO in Algorithm 1. If the updated P_b has not fall within the limits of P_b^{min} and P_b^{max}; then, generate P_b randomly between P_b^{min} and P_b^{max}. Consequently, evaluate E_b by satisfying the BESS constraints given in Equations (9) and (10).

14. Run the load flow and estimate the objective in Equation (3) similar to the step 11.
15. Keep the better candidate solution set of P_b and E_b according to the minimum objective. Moreover, update S and A using Equation (27). Further, determine the candidate that produced the minimum objective and store the values of P_b^{best}, E_b^{best}, and obj_2^{best}.
16. Check $iter^{sub} \leq iter_{max}$. If yes; update $iter^{sub} = iter^{sub} + 1$, and go to step 13. If no; go to step 17.
17. Check $pop^{main} \leq np$. If yes; update $pop^{main} = pop^{main} + 1$, and go to step 5. If no; go to step 18.
18. Update the values of E_r and P_r according to the CHIO in Algorithm 1. If the updated E_r and P_r have not fall within the limits of E_r^{min}, E_r^{max} and P_r^{min}, P_r^{max}, respectively; then, generate E_r and P_r randomly within the limits.
19. Repeat step 6 to step 16 for estimating the optimal P_b, E_b, and obj_2 for new E_r and P_r.
20. Keep the better candidate solution set of E_r and P_r according to the minimum obj_2. Moreover, update S and A using Equation (27). Further, determine the candidate that produced the minimum obj_2 and store them as E_r^{best}, P_r^{best}, P_b^{best}, E_b^{best}, and obj_2^{best}.
21. Check $iter^{main} \leq iter_{max}$. If yes; update $iter^{main} = iter^{main} + 1$, and go to step 18. If no; go to step 22.
22. Check $bc \leq Nbus$. If yes; update $bc = bc + 1$, and go to step 3. If no; go to step 23.
23. Identify the bus location which has the minimum obj_2^{best} and store the parameters corresponding to that location as $E_{r,BLoc}^{best}$, $P_{r,BLoc}^{best}$, $E_{b,BLoc}^{best}$, $P_{b,BLoc}^{best}$, and $obj_{2,BLoc}^{best}$. Where, $BLoc$ is the battery optimal location.

5. Simulation study results and discussions

The main aim of this work is to decrease the APL, RPL and enhance the voltage profile of the PDS by discovering the optimal ratings of SPVDG and BESS at optimal locations in the PDS. The proposed approach is investigated and evaluated in a SONY laptop with Windows 10 configuration, 8GB of RAM, and an Intel Core i3 processor with 2.40 GHz in the MATLAB environment. To examine the effectiveness of the suggested approach, two conventional radial PDSs, viz., 33 and 69 bus systems are investigated. When sizing the SPVDG, the fraction of normalized load on the system when the SPVDG normalized generation has a maximum is considered for the study. It is observed that the SPVDG has the peak at the 85^{th} hour from Figure 3b; therefore, the load fraction corresponding to the 85^{th} hour from the normalized load curve in Figure 3a is considered the load for the study of SPVDG optimal sizing using the proposed methodology. The battery optimal scheduling of charge/discharge of powers is obtained along with the optimal energy rating and power rating considering the variation of load and SPVDG generation for a year. This is modeled by using the suggested methodology for the abovementioned objectives. The technical and algorithm data utilized in this work is as shown in Table 1. In this article, different cases which are based on with and without SPVDG and BESS in the PDS are presented. Moreover, the obtained numerical results demonstrated the proposed method's validity and effectiveness.

5.1. Test system-1: 33 bus radial PDS

The 33 bus PDS works at a voltage of 12.66 kV with a capacity of 100 kVA. It accommodates 33 buses and 32 branches. It contains a total active and reactive power load of 3715 kW and 2300 kVAr, respectively. Table 2 summarizes all the simulated outcomes for the aforementioned case studies such as with and without SPVDG and BESS. It is observed that from the base case, the voltage of 0.9131 p.u. at bus-18 is the lowest nodal voltage among all the nodal voltages. The optimal rating of SPVDG is estimated as 2604.32 kW at bus-8 by using the suggested CHIO algorithm. With the addition of this rated SPVDG in the PDS at the optimal location, the

lowest nodal voltage has been increased to 0.9721 p.u. at bus-18. Moreover, it is also observed from Figure 4 that the deviation of voltages from the unity has also been decreased by the addition of SPVDG in the PDS by following the proposed method. Furthermore, the APL and RPL have been decreased to 95.236 kW and 74.34 kVAr, respectively. The inclusion of BESS, in addition to the SPVDG in the PDS, at the optimal location (bus-29) with the optimal energy rating (2754.46 kWh) and power rating (1350.88 kW) furthermore reduced the APL and RPL to 87.53 kW and 70.20 kVAr, respectively. The lowest nodal voltage of the PDS at the hour when the SPVDG generation has the peak is further enhanced to 0.9762 at the bus-18. It is noted that the APL, RPL, and VD of the system are significantly reduced for the case where both DG and BESS are optimally located with optimal ratings compared to without DG and BESS (i.e. base case). The APL is reduced from 202.68 kW to 87.53 kW with a reduction of 56.81%; similarly, RPL is decreased to 70.20 kVAr from 135.14 kVAr with a reduction of 48.05%. Moreover, the least voltage is improved from 0.9131 p.u. at bus-18 to 0.9762 at bus-18.

Table 1. Technical and algorithm parameters data.

Technical parameters		Algorithm parameters	
Parameter	Value	Parameter	Value
V^{min}, V^{max} (p.u.) [11]	0.95, 1.05	np	40
C_1, C_2	1, 1	$iter_{max}$	500
P^{DGmin}, P^{DGmax} (MW)	0.3, 3	RR [22]	0.05
E_b^{min}, E_b^{max} (kWh)	500, 4000	N_0 [22]	1
P_b^{min}, P_b^{max} (kW)	100, 1000	AGE_{max} [22]	100
SOC^{min}, SOC^{max}, $SOC^{initial}$	0.2, 0.9, and 0.2		
T, T_s (hrs) [23]	24, 96		
η_d, η_c [23]	0.85, 0.85		

Table 2. Simulation results of OPP of PDS with SPVDG and BESS for test system-1.

Parameters	Base case	With only SPVDG	With SPVDG+BESS
P^{DG} @bus, (MW)	-	2.60@8	2.60@8
E_r, P_r (MWh, MW)	-	-	2.75, 1.35 @29
Energy loss, (MWh)	1227.7	966.25	902.85
APL, (kW)	202.68	95.24	87.53
RPL, (kVAr)	135.14	74.34	70.2
Min. voltage @bus, (p.u.)	0.9131@18	0.9721@18	0.9762@18
Max. voltage @bus, (p.u.)	1@1	1@1	1@1
% reduction in Energy loss	-	21.30	26.46
% reduction in APL	-	53.01	56.81
% reduction in RPL	-	44.99	48.05

5.2. Test system-2: 69 bus radial PDS

In this test case, the 69 bus PDS works at an operating voltage of 12.66 kV and a capacity of 100 kVA is studied. It has 69 buses and 68 branches. Moreover, it contains an overall active power load of 3791.89 kW and a reactive power load of 2694.1 kVAr. Similar to test system-1, all the cases are examined on this system, and the results are reported in Table 3.

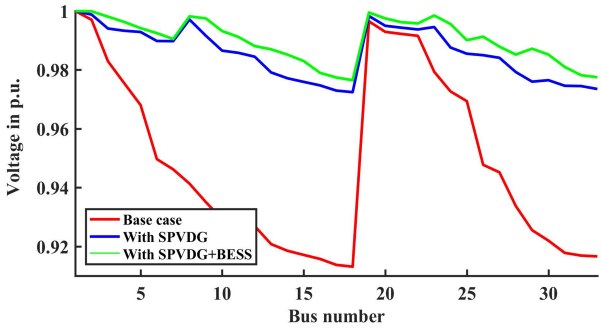

Figure 4. Voltage profile of test system-1 for different case studies

From the base case in Table 3, it is seen that the least voltage of 0.9092 p.u. in the PDS is at bus-65. The optimal peak SPVDG size is estimated for this system as 2053.03 kW at bus-61 using the proposed CHIO algorithm. The addition of this SPVDG into the PDS considerably improved the least voltage of the system to 0.9724 at bus-27. Furthermore, the nodal voltages at all the buses have been improved with the addition of the optimal-sized SPVDG. This can be observed in Figure 5.

Table 3. Simulation results of OPP of PDS with SPVDG and BESS for test system-2.

Parameters	Base case	With only SPVDG	With SPVDG+BESS
P^{DG}@bus (MW)	-	2.05@61	2.05@61
E_r, P_r @bus (MWh, MW)	-	-	3.75 , 1.17 @64
Energy loss, (MWh)	1358.4	999.18	959.37
APL, kW	224.95	75.08	69.35
RPL, kVAr	102.14	35.90	32.10
Min. voltage @bus (p.u.)	0.9092@65	0.9724@27	0.9769@27
Max. voltage @bus (p.u.)	1@1	1@1	1@1
% reduction in Energy loss	-	26.44	29.38
% reduction in APL	-	66.62	69.17
% reduction in RPL	-	64.86	68.57

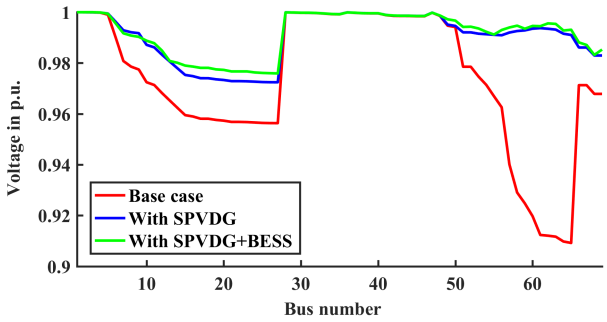

Figure 5. Voltage profile of test system-2 for different case studies.

Moreover, with the inclusion of this SPVDG, the APL and RPL of the PDS have been significantly reduced to 75.08 kW and 35.90 kVAr, respectively. The integration of BESS besides SPVDG in the PDS at the

optimum bus location (bus-64) with the optimal energy rating (3750.48 kWh) and power rating (1168.41 kW) drastically curtailed the APL and RPL even further to 69.35 kW and 32.10 kVAr, with a percentage reduction of 69.17% and 68.57%, respectively. Furthermore, the least voltage of the PDS at the hour when the SPVDG generation has the peak has been notably enhanced to 0.9769 at bus-27. Similar to the case of the 33 bus system, it is observed that the system's APL, RPL, and VD are greatly lowered when both DG and BESS are optimally situated with optimal ratings, as opposed to when neither DG nor BESS is present in the PDS (i.e. base case).

Lastly, the proposed method is compared with the well-known metaheuristic methods such as GA, grey wolf optimization (GWO), PSO, enhanced leader PSO (ELPSO), Jaya algorithm (JA), and enhanced elephant herding algorithm (EEHA). These algorithms are implemented for the present study for both the test systems and tabulated the obtained results in Table 4. It is observed that the results obtained by using the suggested algorithm has significantly improved the objectives when compared to the remaining algorithms.

Table 4. Comparison of proposed method with different algorithms for OPP of PDS.

Bus system	Case study	Algorithm	Energy loss (MWh)	APL (kW)	RPL (kVAr)	Min. voltage (p.u.)
33	With SPVDG	GA (studied)	1080.37	111.27	84.19	0.9650
		GWO (studied)	1062.13	110.56	83.99	0.9658
		PSO (studied)	996.78	103.59	81.26	0.9705
		ELPSO (studied)	981.22	102.47	79.81	0.9714
		JA (studied)	977.63	101.49	79.45	0.9714
		EEHA (studied)	978.04	101.08	78.91	0.9714
		Proposed method	**966.25**	**95.24**	**74.34**	**0.9721**
	With SPVDG+BESS	GA (studied)	1011.92	105.32	80.35	0.9689
		GWO (studied)	1002.86	103.25	80.12	0.9690
		PSO (studied)	967.76	95.24	76.98	0.9721
		ELPSO (studied)	915.31	91.92	75.69	0.9743
		JA (studied)	913.12	91.26	75.56	0.9743
		EEHA (studied)	911.51	90.84	74.28	0.9750
		Proposed method	**902.85**	**87.53**	**70.2**	**0.9762**
69	With SPVDG	GA (studied)	1121.76	98.23	52.12	0.9653
		GWO (studied)	1075.94	95.59	51.02	0.9661
		PSO (studied)	1039.45	80.69	45.6	0.9709
		ELPSO (studied)	1020.96	78.9	42.62	0.9716
		JA (studied)	1015.95	77.9	42.05	0.9717
		EEHA (studied)	1010.41	76.67	40.68	0.9719
		Proposed method	**999.18**	**75.08**	**35.9**	**0.9724**
	With SPVDG+BESS	GA (studied)	1089.23	85.83	49.27	0.9662
		GWO (studied)	1024.71	81.73	45.09	0.9668
		PSO (studied)	981.68	75.71	40.03	0.9749
		ELPSO (studied)	965.59	72.35	39.53	0.9751
		JA (studied)	964.94	72.01	38.96	0.9753
		EEHA (studied)	963.45	71.73	36.32	0.9755
		Proposed method	**959.37**	**69.35**	**32.1**	**0.9769**

6. Conclusion

A novel CHIO optimization technique is successfully implemented in this article for the OPP of the PDS. This algorithm is efficiently controlled by the reproduction rate and maximum age factors for global exploration and local exploitation for identifying the optimal solution. The proposed algorithm is studied to determine the optimal location and optimal size of the SPVDG and BESS in the PDS for diminishing APL, RPL, and VD, thereby improving the voltage profile. The supremacy of the developed algorithm is highlighted by successfully employing it on the two test PDSs viz., 33 and 69 bus PDSs. Various case studies predicated on with and without SPVDG and BESS are simulated. The numerical outcomes of APL, RPL, minimum voltage, and maximum voltage of the PDS that are based on a comparative analysis of all the case studies are tabulated. The case where both SPVDG and BESS are integrated into the PDS at the optimal location with optimal size has provided significant improvement in the percentage curtailment of APL and RPL for both 33 and 69 bus systems. Furthermore, in this case, the voltage profile has also been near unity at all buses for both the PDSs along with the improvement in the least voltage. Lastly, the dominance of the suggested algorithm to achieve the near-optimal global solution in comparison with other existing algorithms such as GA, GWO, PSO, and ELPSO are evident and the results are tabulated. Although this topic is explored under normal generation and load conditions, an extension of this article for future work can include multiple objectives in an uncertain load and generation environment.

References

[1] Jayasekara N, Masoum MAS, Wolfs PJ. Optimal operation of distributed energy storage systems to improve distribution network load and generation hosting capability. IEEE Transactions on Sustainable Energy 2016; 7 (1): 250–261. doi: 10.1109/TSTE.2015.2487360

[2] Bayat A, Bagheri A. Optimal active and reactive power allocation in distribution networks using a novel heuristic approach. Applied Energy 2019; 233: 71-85. doi: 10.1016/J.APENERGY.2018.10.030

[3] Foster JD, Berry AM, Boland N, Waterer H. Comparison of mixed-integer programming and genetic algorithm methods for distributed generation planning. IEEE Transactions on Power Systems 2014; 29 (2): 833-843. doi: 10.1109/TPWRS.2013.2287880

[4] Garfi O, Aloui H. Multiple distributed generations placement and sizing based on voltage stability index and power loss minimization. Turkish Journal of Electrical Engineering and Computer Sciences 2019; 27 (6): 4567-4579. doi: 10.3906/elk-1812-45

[5] Purlu M, Turkay BE. Optimal allocation of renewable distributed generations using heuristic methods to minimize annual energy losses and voltage deviation index. IEEE Access 2022; 10: 21455-21474. doi: 10.1109/ACCESS.2022.3153042

[6] Hien NC, Mithulananthan N, Bansal RC. Location and sizing of distributed generation units for loadabilty enhancement in primary feeder. IEEE Systems Journal 2013; 7 (4): 797-806. doi: 10.1109/JSYST.2012.2234396

[7] Kadir AF, Mohamed A, Shareef H, WANIK MZ. Optimal placement and sizing of distributed generations in distribution systems for minimizing losses and THD using evolutionary programming. Turkish Journal of Electrical Engineering and Computer Sciences 2013; 21 (8): 2269-82. doi: 10.3906/elk-1205-35

[8] Abou El-Ela AA, El-Sehiemy RA, Abbas AS. Optimal placement and sizing of distributed generation and capacitor banks in distribution systems using water cycle algorithm. IEEE Systems Journal 2018; 12 (4): 3629-3636. doi: 10.1109/JSYST.2018.2796847

[9] Ankush R, Rama P. Application of jaya algorithm in finding optimal placement and sizing of distributed generation units. International Journal of Emerging Trends in Engineering Research 2020; 8 (10): 7625-7633. doi: 10.30534/ijeter/2020/1528102020

[10] Nand KM, Sonam P, Anil S, Nikhil G, Khaleequr RN. Improved elephant herding optimization for multiobjective DER accommodation in distribution systems. IEEE Transactions on Industrial Informatics 2018; 14(3): 1029-1039. doi: 10.1109/TII.2017.2748220

[11] Abu-Mouti FS, El-Hawary ME. Optimal distributed generation allocation and sizing in distribution systems via artificial bee colony algorithm. IEEE transactions on power delivery 2011; 26 (4): 2090-2101. doi: 10.1109/TPWRD.2011.2158246

[12] Kamel S, Awad A, Abdel-Mawgoud H, Jurado F. Optimal DG allocation for enhancing voltage stability and minimizing power loss using hybrid gray wolf optimizer. Turkish Journal of Electrical Engineering and Computer Sciences 2019; 27 (4): 2947-2961. doi: 10.3906/elk-1805-66

[13] Farh HM, Al-Shaalan AM, Eltamaly AM, Al-Shamma'A AA. A novel crow search algorithm auto-drive PSO for optimal allocation and sizing of renewable distributed generation. IEEE Access 2020; 8: 27807-27820. doi: 10.1109/ACCESS.2020.2968462

[14] Prakash P, Khatod DK. Optimal sizing and siting techniques for distributed generation in distribution systems: A review. Renewable and sustainable energy reviews 2016;57: 111-130. doi: 10.1016/J.RSER.2015.12.099

[15] Yang Y, Bremner S, Menictas C, Kay M. Battery energy storage system size determination in renewable energy systems: A review. Renewable and Sustainable Energy Reviews 2018; 91: 109-125. doi: 10.1016/J.RSER.2018.03.047

[16] Vykhodtsev AV, Jang D, Wang Q, Rosehart W, Zareipour H. A review of modelling approaches to characterize lithium-ion battery energy storage systems in techno-economic analyses of power systems. Renewable and Sustainable Energy Reviews 2022; 166: 112584. doi: 10.1016/J.RSER.2022.112584

[17] Ekren O, Ekren BY. Size optimization of a PV/wind hybrid energy conversion system with battery storage using simulated annealing. Applied energy 2010; 87 (2): 592-598. doi: 10.1016/J.APENERGY.2009.05.022

[18] Dong X, Bao G, Lu Z, Yuan Z, Lu C. Optimal battery energy storage system charge scheduling for peak shaving application considering battery lifetime. In: Springer 2011 Informatics in Control, Automation and Robotics Conference; Berlin, Heidelberg; 2011. pp. 211-218.

[19] Khasanov M, Kamel S, Awad A, Jurado F. Optimal planning DG and BES units in distribution system considering uncertainty of power generation and time-varying load. Turkish Journal of Electrical Engineering and Computer Sciences 2021; 29 (2): 773-795. doi: 10.3906/elk-2003-46

[20] Khasanov M, Kamel S, Rahmann C, Hasanien HM, Al-Durra A. Optimal distributed generation and battery energy storage units integration in distribution systems considering power generation uncertainty. IET Generation, Transmission & Distribution 2021; 15 (24): 3400-3422. doi: 10.1049/GTD2.12230

[21] Nayak CK, Nayak MR. Techno economic analysis of a grid-connected PV and battery energy storage system considering time of use pricing. Turkish Journal of Electrical Engineering and Computer Sciences 2018; 26 (1): 318-329. doi: 10.3906/elk-1703-35

[22] Al-Betar MA, Alyasseri ZA, Awadallah MA, Abu Doush I. Coronavirus herd immunity optimizer (CHIO). Neural Computing and Applications 2021; 33 (10): 5011-5042. doi: 10.1007/S00521-020-05296-6/TABLES/16

[23] Mukhopadhyay B, Das D. Multi-objective dynamic and static reconfiguration with optimized allocation of PV-DG and battery energy storage system. Renewable and sustainable energy reviews 2020; 124: 109777. doi: 10.1016/J.RSER.2020.109777

[24] Kanwar N, Gupta N, Niazi KR, Swarnkar A, Bansal RC. Simultaneous allocation of distributed energy resource using improved particle swarm optimization. Applied Energy 2017; 185: 1684-1693. doi: 10.1016/J.APENERGY.2016.01.093

[25] Teng JH. A direct approach for distribution system load flow solutions. IEEE Transactions on power delivery 2003; 18 (3): 882-887. doi: 10.1109/TPWRD.2003.813818